Journal of Alloys and Compounds 509 (2011) 8251–8255

Contents lists available at ScienceDirect

Journal of Alloys and Compounds

journal homepage: www.elsevier.com/locate/jallcom

Structure and dielectric constant of silver molybdophosphate mixed network former glasses

B. Deb, A. Ghosh*

Department of Solid State Physics, Indian Association for the Cultivation of Science, Jadavpur, Kolkata 700032, India

ARTICLE INFO

Article history:
Received 11 April 2011
Received in revised form 23 May 2011
Accepted 25 May 2011
Available online 6 June 2011

Keywords:
Amorphous materials
FTIR spectra
Dielectric constant

ABSTRACT

Structure and dielectric constant of silver molybdophosphate mixed network former glasses have been reported in this paper. The Fourier transform infrared (FTIR) spectroscopy has been used to investigate the effect of MoO_3 on the glass network structure. The existence of characteristic absorption bands corresponding to the vibration of P═O bond, P–O^- mode and P–O–P bond and the presence of MoO_4^{2-} anions have been ascertained from the FTIR spectra. It is observed that the increase of MoO_3 content in the compositions changes the network structure by creating non-bridging oxygen caused by the breaking of long phosphate chains. It is further observed that the dielectric constant and dielectric strength of these glasses increases with the increase of MoO_3 content, which is attributed to the increase of the polarizability of the glasses due to addition of MoO_3.

1. Introduction

Ion conducting materials continue to be a matter of great interest for their potential applications in optical devices, electrochemical devices, e.g., electrochromic display, in sensors [1–8]. They are equally important from scientific point of view to understand the structure–transport correlation in glasses [9–11]. In particular, the study of P_2O_5 based glasses are interesting because of their superior physical properties such as high thermal expansion coefficients, low melting temperature, low softening temperature and low transition temperature [12–15]. Tunability of various characteristics such as mechanical, dielectric, thermal properties can be achieved in glasses, which contain more than one network former compared to the single network former glasses. Studies of few mixed former glass systems containing phosphate, molybdate, etc. with other glass network formers have been reported [16–20].

The different properties, such as thermal, mechanical, electrical of mixed network former glasses are significantly different from those of single network former glasses and these changes can be attributed to the change of microscopic structure of the glasses [11,21,22]. The network of the vitreous P_2O_5 is formed from PO_4 tetrahedra, which are connected through P–O–P linkages forming a polymeric structure. The addition of other glass formers can change the characteristics of the phosphate network by altering the network connectivity. The extent of structural modification in such glasses strongly depends on the glass compositions and on the nature of network formers. MoO_3 is a non-traditional glass former and acts both as a network former as well as a network modifier depending upon its concentration in the glassy matrices [23–26]. Addition of high MoO_3 concentration in phosphate glass leads to the formation of various molybdenum units that enter into the glass network by cross-linking phosphate chains [23,24]. Infrared spectroscopic investigation of a few PbO modified molybdophosphate glasses reveals that the addition of the modifier de-polymerizes the phosphorous–oxygen chain by forming new P–O–Pb bonds and non-bridging oxygen in the network [27]. A few studies of compositional dependence glass network structure in a few molybdophosphate glasses show that the increase of MoO_3 content leads to the transformation of Mo–O^- and P═O bonds into Mo–O–Mo and weaker Mo–O–P bridging bonds [28,29]. In zinc phosphate and borophosphate glasses [30,31] it has been observed that the incorporation of MoO_3 increases the depolymerization of phosphate chains and a gradual transformation of metaphosphate into diphosphate and orthophosphate units occurs. The Raman spectroscopic study of these glasses reveals that the ratio of MoO_6/MoO_4 increases with increasing content of MoO_3 [32,33]. The addition of MoO_3 thus affects the network stability of glasses: the stability of network is higher for low MoO_3 content, whereas at higher MoO_3 content the network structure becomes weak and is more prone to crystallization due to formation of MoO_6 clusters. From structural point of view it is thus challenging to study the glass network structure in a system consisting of one typical glass network former (P_2O_5) and other conditional network former (MoO_3) and the consequent effects of substituting one former by another.

In this work, we have focused our attention to study the effect of incorporation of MoO_3 in silver phosphate glass. The addition of

* Corresponding author. Tel.: +91 3324734971; fax: +91 3324732805.
E-mail address: sspag@iacs.res.in (A. Ghosh).

0925-8388/$ – see front matter © 2011 Elsevier B.V. All rights reserved.
doi:10.1016/j.jallcom.2011.05.098

MoO_3 is observed to affect the glass network structure depending on composition. The effect of addition of MoO_3 on the dielectric properties of the glasses has been also studied. This work thus sheds some light on the structure and dielectric properties of MoO_3 containing silver phosphate glasses.

2. Experimental details

The glass samples of compositions $yAg_2O–(1-y)(xMoO_3–(1-x)P_2O_5)$ where $0 \leq x \geq 0.90$ and $y = 0.30$ and 0.40 were prepared by conventional melt quenching technique. The reagent grade chemicals $AgNO_3$, MoO_3 and $NH_4H_2PO_4$ were thoroughly mixed in appropriate proportion. The mixtures were heated in an alumina crucible at 400 °C for 4 h for denitrogenation of $AgNO_3$. The mixtures were then melted in the temperature range of 800–900 °C depending on composition and equilibrated for 2 h. The melts were then rapidly quenched between two aluminum plates to obtain the desired glass samples.

The formation of glasses was ascertained from X-ray diffraction (XRD) using a X-ray diffractometer (Bruker, model D8 Advanced AXS) using Cu K_α radiation ($\lambda = 1.54$ Å). The density of the glass samples at room temperature was determined using Archimedes principle using acetone as the immersion liquid. The differential scanning calorimetry (DSC) traces of the samples were recorded using a differential scanning calorimeter (TA instruments, model - DSC Q2000) in N_2 environment at a constant heating rate of 10 °C/min. The FTIR spectra of the powder samples in KBr matrix in the ratio 1:100 were recorded at room temperature using a FTIR spectrometer (SHIMADZU, model FTIR-8400S). The dielectric data of the samples were measured in an LCR meter (Quad Tech, model 7600) in the frequency range of 10 Hz–2 MHz and in a wide temperature range.

3. Results and discussion

Fig. 1 shows the X-ray diffraction patterns for several compositions. The patterns show characteristic wide haloes, which indicate the amorphous nature of the as-prepared samples. Table 1 summarizes the value of different parameters calculated for all glass compositions. It is noted in Table 1 that the density of the glasses at a fixed Ag_2O content gradually increases with increase of MoO_3 content whereas the molar volume decreases. The composition dependence of density and molar volume depends largely on the molecular weight of the replaced oxide and on the change of number of atoms. Thus, the observed trends in the change in the density and the molar volume is attributed to the partial replacement of a low molecular weight and low density P_2O_5 ($M = 141.945$ g mol^{-1}, $\rho = 2.39$ g cm^{-3}) by a high molecular weight and high density MoO_3 ($M = 143.94$ g mol^{-1}, $\rho = 4.69$ g cm^{-3}).

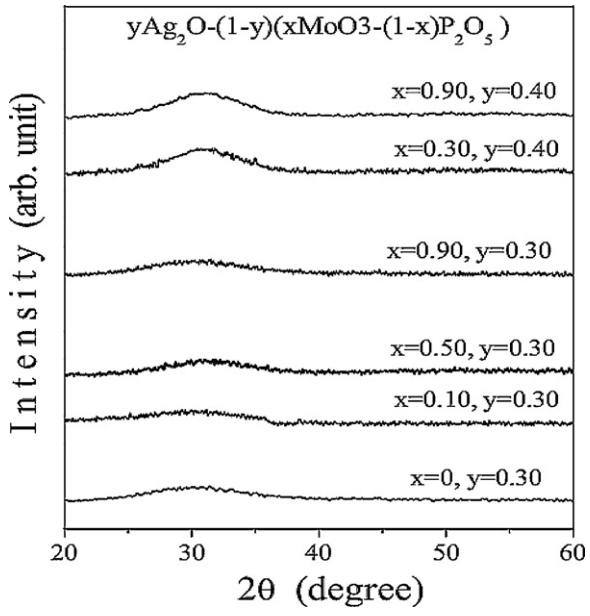

Fig. 1. The XRD patterns for several glass samples of composition $yAg_2O–(1-y)(xMoO_3–(1-x)P_2O_5)$.

Table 1
The value of the density (ρ), molar volume (V_m), glass transition temperature (T_g), average cross link density ($\langle n_c \rangle$) and the oxide ion polarizability ($\alpha_{O^{2-}}$) for the glasses of compositions $yAg_2O–(1-y)(xMoO_3–(1-x)P_2O_5)$.

Composition	ρ (g cm^{-3}) (±0.05)	V_m (cm^3 mol^{-1})	T_g (°C) (±10)	$\langle n_c \rangle$	$\alpha_{O^{2-}}$ (Å^3)
$y = 0.30$					
$x = 0$	3.76	44.83	272	1.30	1.57
$x = 0.10$	4.34	38.94	250	1.38	1.59
$x = 0.30$	4.52	37.45	275	1.57	1.63
$x = 0.50$	4.65	36.49	285	1.79	1.67
$x = 0.70$	5.35	31.56	343	2.04	1.72
$x = 0.90$	5.48	31.04	266	2.36	1.77
$y = 0.40$					
$x = 0$	4.14	42.97	253	1.40	1.72
$x = 0.10$	4.36	40.82	220	1.47	1.74
$x = 0.30$	4.61	38.65	267	1.64	1.78
$x = 0.50$	4.87	36.64	278	1.82	1.83
$x = 0.70$	5.52	32.37	298	2.04	1.87
$x = 0.90$	6.22	28.76	230	2.28	1.92

The differential scanning calorimetry (DSC) traces for several glass compositions are shown in Fig. 2. The DSC curves show endothermic baseline shifts indicative of the glass transition followed by the exothermic crystalline peaks. It is noted that with increasing MoO_3 content the intensity of crystallization peaks increases, signifying an increasing tendency of crystallization. Fig. 3(a) shows the variation of glass transition temperature (T_g) with MoO_3 content. It is observed that the glass transition temperature initially shows an increasing trend with increasing MoO_3 content, but it decreases at higher MoO_3 content. The glass transition temperature, T_g is a structure sensitive parameter depending predominantly on the bond strength, degree of cross-link density and closeness of packing. We have calculated a structural parameter called the cross-link density (n_c) which is defined as the number of bridging oxygen atoms per network-forming atom. The value of n_c for Ag_2O, MoO_3 and P_2O_5 are two, three and one, respectively [34]. The average cross link density $\langle n_c \rangle$ is then calculated from

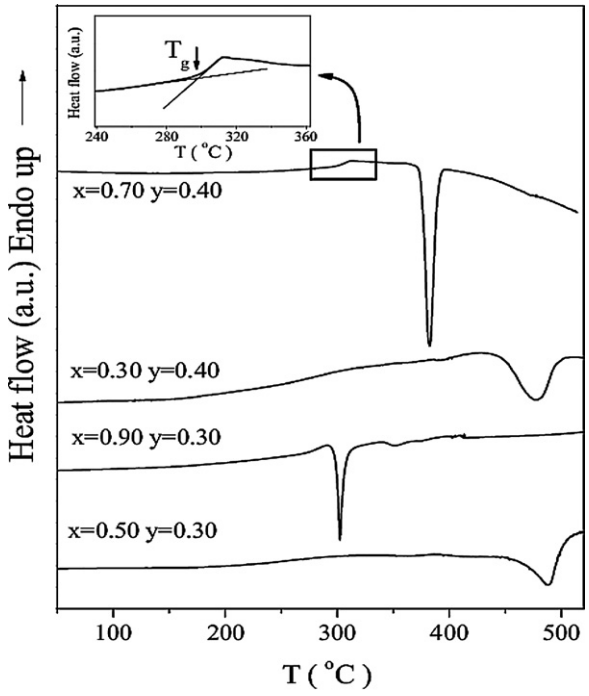

Fig. 2. DSC traces for several glasses of composition $yAg_2O–(1-y)(xMoO_3–(1-x)P_2O_5)$ shown. The inset shows the zoomed in portion of the selected area indicating the endothermic baseline shift and the determination of T_g.

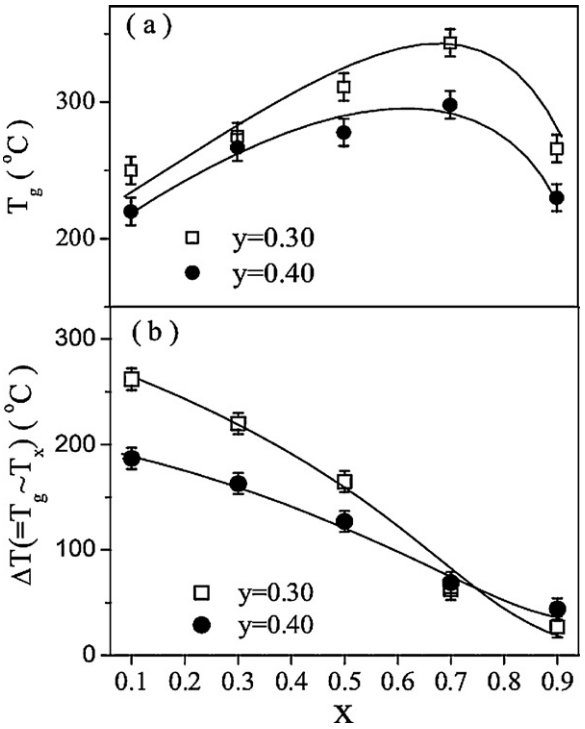

Fig. 3. (a) Variation of glass transition temperature, T_g with MoO_3 content for the glass samples of compositions yAg_2O–$(1-y)(xMoO_3$–$(1-x)P_2O_5)$. (b) The variation of thermal stability, ΔT with MoO_3 content for all the glass samples. Lines are drawn as a guide to the eye and error bars are also shown in both the figures.

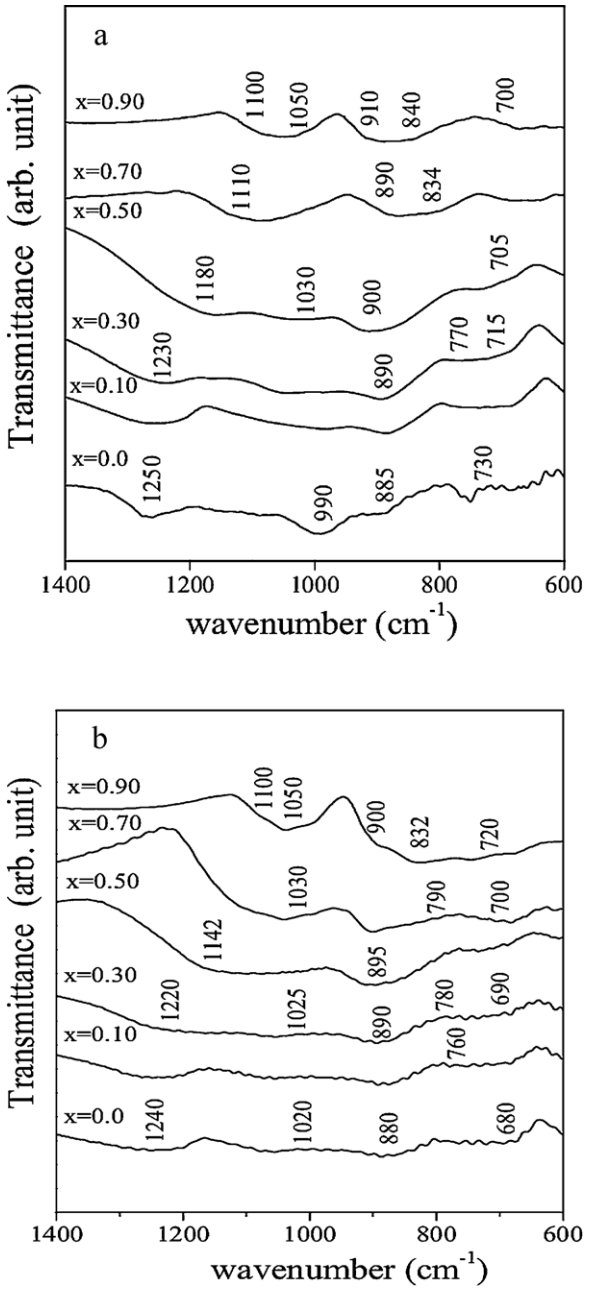

Fig. 4. FTIR spectra for the glass samples of compositions (a) $0.30Ag_2O$–$0.70(xMoO_3$–$(1-x)P_2O_5)$ and (b) $0.40Ag_2O$–$0.60(xMoO_3$–$(1-x)P_2O_5)$.

glass composition by adding the contribution of respective compound. It is noted in Table 1 that the average cross link density $\langle n_c \rangle$ of the glasses increases with the increase of MoO_3 content, which is due to the replacement of low cross-link density network former P_2O_5 by high cross-link density network former MoO_3. The initial increase of T_g with increasing MoO_3 content is thus attributed to the increasing cross-link density of the glass network. On the other hand, the bond strength of Mo–O bond (560.2 kJ/mol) is less than that of P–O bond (599.1 kJ/mol), so that the mean bond strength in MoO_3–P_2O_5 glasses decreases with an increase in the MoO_3 content. Here, for lower MoO_3 content the cross-link density dominates increasing the network connectivity and increasing T_g. But, for higher MoO_3 content the weakening of glass structure occurs due to the decrease in bond strength which decreases T_g. Thus, the occurrence of T_g maximum can be envisaged as the competition between the increase of the cross-link density and the decrease of the mean bond strength, the former being dominant at lower MoO_3 content and later at higher MoO_3 content.

The difference, ΔT between the glass transition temperature (T_g) and crystallization onset temperature (T_x), can be considered as an indicative of the thermal stability of the glasses. Fig. 3(b) shows the composition dependence of ΔT, which clearly shows that the thermal stability decreases with increasing MoO_3 content. The decrease of thermal stability of the glasses can be attributed to the increase of depolymerization or the breaking of the network chain structure of the phosphate network with increasing MoO_3 content as revealed from FTIR spectra discussed in the following paragraph.

The FTIR spectra for different glass compositions are shown in Fig. 4(a) and (b) for two series. The spectra reveal different characteristic absorption bands corresponding to different vibration modes of phosphate and molybdate units. The bands in the region 1100–1250 cm^{-1}, 990–1050 cm^{-1}, 880–920 cm^{-1} and 680–740 cm^{-1} are assigned to the asymmetric stretching vibration of P=O bond, asymmetric stretching vibration of P–O$^-$ mode, asymmetric stretching mode of P–O–P bond and symmetric stretching of P–O–P bond respectively [28–31]. The band observed around 750–840 cm^{-1} for glasses containing MoO_3 is assigned to the stretching vibration of MoO_4^{2-} anions [35]. The relative intensity of different bands changes with composition. The FTIR spectra of pure phosphate glasses reveal that the glasses are made up of chains of $(PO_3^-)_n$ and in part by corner shared chains of $(PO_3^-)_n$, in a two and three dimensional networks. It is noted that the absorption band around 890 cm^{-1} and 680 cm^{-1} corresponding to asymmetric and symmetric stretching vibration of P–O–P bond shifts slightly towards higher wave number with increasing MoO_3 content. The absorption band observed around 1250 cm^{-1} shifts towards lower wave number, whereas that around 1020 cm^{-1} shifts towards higher wave number with increase of MoO_3 content. This change

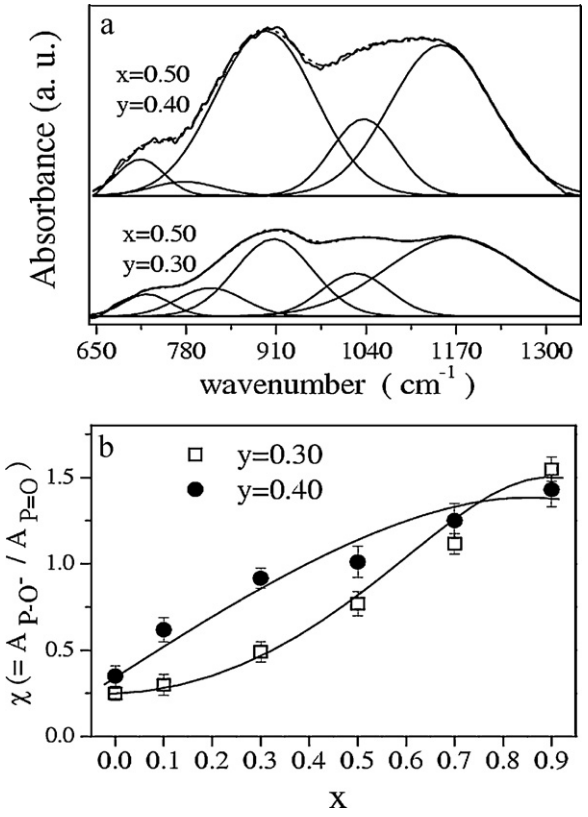

Fig. 5. (a) The deconvulution of FTIR spectra for glass samples of compositions yAg_2O–$(1-y)(0.50MoO_3$–$0.50P_2O_5)$ for $y = 0.30$ and $y = 0.40$. The deconvuluted bands are also shown. (b) The variation of the ratio of the relative area of the concentration of P–O$^-$ vibrational mode to P=O vibrational mode (χ) with MoO_3 content for the glass system of compositions yAg_2O–$(1-y)(xMoO_3$–$(1-x)P_2O_5)$. The solid line is a guide to the eye.

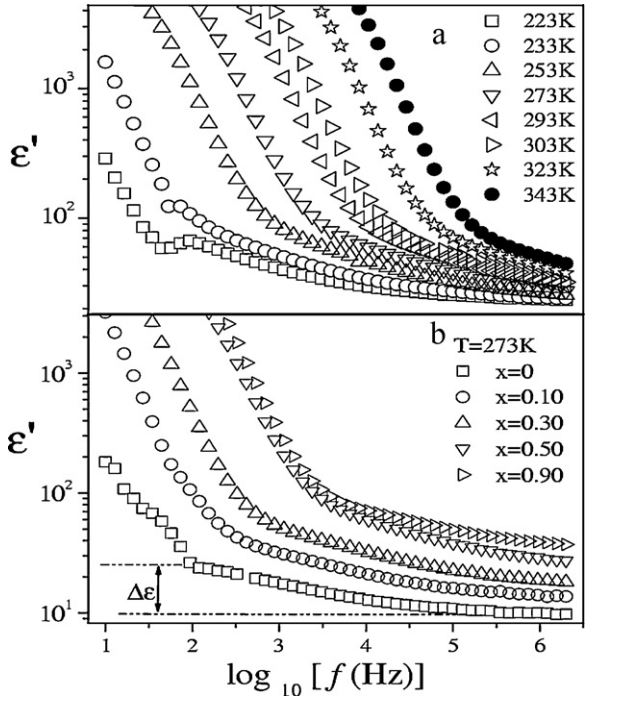

Fig. 6. (a) Frequency dependence of dielectric constant ε' for $0.40Ag_2O$–$0.60(0.50MoO_3$–$0.50P_2O_5)$ glass at several temperatures. (b) Frequency dependence of dielectric constant ε' at 273 K for the different compositions $0.40Ag_2O$–$0.60(xMoO_3$–$(1-x)P_2O_5)$.

of the band position points to the weakening of phosphate network chain by replacement of P–O–P bonds by weaker P–O–Mo bonds with increasing MoO_3 content [32] and in turn suggests the decrease of the number of bridging phosphate oxygen in the glasses. It is also noted that the intensity of P=O vibration mode decreases and that of P–O$^-$ increases with the increase of the MoO_3 content.

To quantify the relative proportion of different vibration modes we have de-convoluted the FTIR spectra as shown in Fig. 5(a). The relative areas of different bands are then obtained as the ratio of the area under the corresponding band to the total area under the entire spectra. Fig. 5(b) shows the variation of the ratio of relative area of P–O$^-$ vibration mode to that of P=O vibration mode. It is observed that the relative area of P=O mode to that of P–O$^-$ mode increases with MoO_3 content, which indicates that the number of non-bridging oxygen units increase in the glasses due to depolymerization of the phosphate chains caused by MoO_3 addition. Addition of MoO_3 to the glass compositions thus causes a gradual degradation of the network and $(PO_3^-)_n$ chains and gives rise to a variety of low-condensed or monomeric phosphate units with higher number of non-bridging oxygen units. Similar results are also obtained from NMR studies for ZnO–MoO_3–P_2O_5 glasses [30], where it is observed that increasing MoO_3 content at the expense of P_2O_5 increases the phosphate units having higher number of non-bridging oxygen units caused by the breaking of long phosphate chain. For the MoO_3 containing glasses, the characteristic absorption band at around 750 cm^{-1} shifts towards higher wave number as MoO_3 increases, indicating the tendency of transformation of MoO_4 units into MoO_6 clusters with high MoO_3 content [31].

Fig. 6(a) shows the frequency dependence of dielectric constant ε' with frequency for a selected composition at several temperatures, while Fig. 6(b) shows the same for different compositions at a particular temperature. From the frequency dependence of ε' (Fig. 6) it is observed that in the high frequency side ε' shows a leveling-off, denoted as ε_∞, which is attributed to the contribution from rapid polarization of atoms and electrons present in the samples under applied electric field. In the intermediate frequency range ε' increases with the decrease in frequency up to certain value, at which a plateau like feature is observed and the value at this level is denoted as ε_s, the low frequency static value. This may be related to the long range hoping motion of ions from one site to the other, where polarization is associated with the changing environment of the different sites, ions hops into [9,10]. The onset of plateau is observed to shift to higher frequency as the temperature is increased. At sufficiently low frequency, ε' increases rapidly due to the additional contribution from electrode and interfacial polarization. It is also noted that the value of ε' increases with the increase in temperature (Fig. 6(a)). The temperature dependence of ε' may be linked to the dipolar polarization, namely the weakening of the intermolecular forces, which increases the orientational polarization.

The dielectric strength, $\Delta\varepsilon$ defined as the difference between low frequency static value (ε_s) and the high frequency limiting value (ε_∞) of the ε', has been obtained from such plots as shown in Fig. 7(b). Fig. 7(a) and (b) show the composition dependence of ε' at a fixed frequency and temperature and the dielectric strength, $\Delta\varepsilon$ respectively. It is noted in Fig. 7(a) that ε' increases with increase in Ag_2O as well as MoO_3 content. The compositional dependence of $\Delta\varepsilon$ shows an increasing trend with increasing MoO_3 content. The increase in dielectric constant as well as dielectric strength may be associated with the increase of polarizability of oxygen ion ($\alpha_{O^{2-}}$) with increasing MoO_3 content as listed in Table 1. The oxygen ion

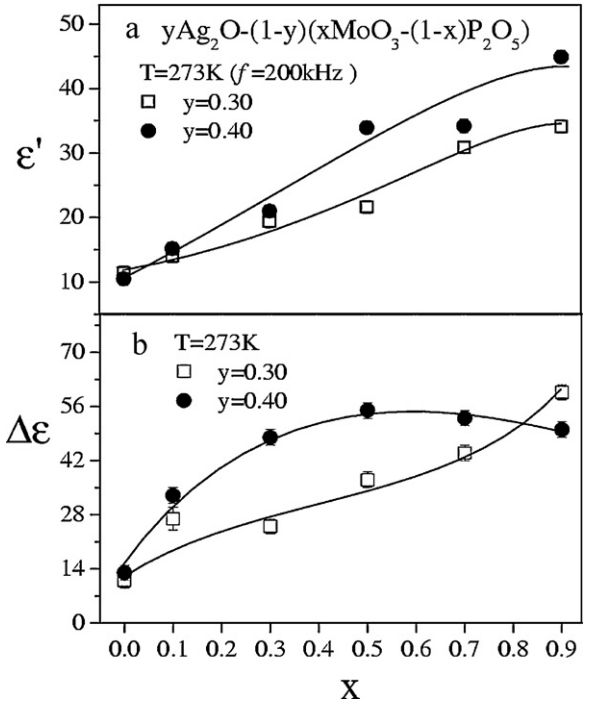

Fig. 7. (a) Composition dependence of ε' at 273 K and at 200 kHz for the glass compositions $y\mathrm{Ag_2O}$–$(1-y)(x\mathrm{MoO_3}$–$(1-x)\mathrm{P_2O_5})$. (b) Composition dependence of dielectric strength, $\Delta\varepsilon$ at 273 K for the glass compositions $y\mathrm{Ag_2O}$–$(1-y)(x\mathrm{MoO_3}$–$(1-x)\mathrm{P_2O_5})$. The lines are drawn as a guide to the eye.

polarizability ($\alpha_{O^{2-}}$) of the glasses has been calculated using the following relation [36]:

$$\alpha_{O^{2-}} = \frac{1.67}{1.67 - \Lambda_{th}},$$

where Λ_{th} represents the theoretical optical basicity. In addition to this, molybdenum ions have also higher polarizability (12.8 Å^3) compared to that of phosphorous ions (3.6 Å^3). The FTIR study also indicates that the increase of MoO_3 content in the compositions increases the breaking of the phosphate network chains by creating more non-bridging oxygen of the phosphate units and this facilitates the ability of the anions to follow the changing electric field to a large extent so that the dielectric constant as well as strength increases.

4. Conclusions

The incorporation of MoO_3 into the silver phosphate glass leads to the structural modification of the phosphate glass network. The characteristic absorption band at ~1250 cm^{-1} corresponding to P=O vibration mode shifts towards lower wave number, whereas that at ~1020 cm^{-1} corresponding to P–O$^-$ absorption band shifts gradually towards higher wave number indicating the increase of depolymerization of the phosphate network with increasing MoO_3 content. The relative area of the P=O vibrational mode to that of P–O$^-$ vibrational mode increases with increase of MoO_3 content, signifying the increase of non-bridging oxygen resulting from depolymerization of the phosphate chains, which also attributes to the increase of the dielectric strength of the glasses with increasing MoO_3. The thermal stability of the glasses decreases with the increase of MoO_3 content.

Acknowledgement

BD thankfully acknowledge CSIR for a research fellowship (via award no. 09/080(0564)/2007-EMR-I).

References

[1] J. Maier, Nat. Mater. 4 (2005) 805–815.
[2] M.A. Samee, A.M. Awasthi, T. Shripathi, S. Bale, Ch. Srinivasu, S. Rahman, J. Alloys Compd. 509 (2011) 3183–3189.
[3] P. Boolchand, W.J. Bresser, Nature 410 (2001) 1070–1073.
[4] J.M.C. Garrido, M.A. Urena, B. Arcondo, J. Alloys Compd. 495 (2010) 356–359.
[5] P. Vinatier, Y. Hamon, in: S. Baranovski (Ed.), Charge Transport in Disordered Solids with Applications in Electronics, John Wiley & Sons, England, 2006 (Chapter 11).
[6] R. Praveena, K.H. Jang, C.K. Jayasankar, H.J. Seo, J. Alloys Compd. 496 (2010) 335–340.
[7] A. Kermaoui, F. Pelle, J. Alloys Compd. 469 (2009) 601–608.
[8] A. Aboulaich, D.E. Conte, J.O. Fourcade, C. Jordy, P. Willmann, J.C. Jumas, J. Power Sources 195 (2010) 3316–3322.
[9] J.C. Dyre, P. Maass, B. Roling, D.L. Sidebottom, Rep. Prog. Phys. 72 (2009) 046501.
[10] D.L. Sidebottom, Rev. Mod. Phys. 81 (2009) 999–1014.
[11] P. Mustarelli, L. Linati, V. Tartara, C. Tomasi, A. Magistris, Solid State Nucl. Magn. Reson. 27 (2005) 112–121.
[12] S.C. Colak, E. Aral, J. Alloys Compd. 509 (2011) 4935–4939.
[13] J. Hong, D. Zhao, J. Gao, M. He, H. Li, G. He, J. Non-Cryst. Solids 356 (2010) 1400–1403.
[14] A.E. Marino, S.R. Arrasmith, L.L. Gregg, S.D. Jacobs, G. Chen, Y. Duc, J. Non Cryst. Solids 289 (2001) 37–41.
[15] R.K. Brow, D.R. Tallant, J. Non Cryst. Solids 222 (1997) 396–406.
[16] Y.B. Saddeek, K.A. Aly, A. Dahshan, I.M.El. Kashef, J. Alloys Compd. 494 (2010) 210–213.
[17] B. Eraiah, R.V. Anavekar, J. Alloys Compd. 489 (2010) 325–327.
[18] P. Mosner, K. Vosejpková, L. Koudelka, L. Montagne, B. Revel, J. Non-Cryst. Solids 357 (2011) 2648–2652.
[19] S. Rada, M. Culea, M. Rada, T. Rusu, E. Culea, J. Alloys Compd. 490 (2010) 270–276.
[20] P. Mosner, K. Vosejpková, L. Koudelka, L. Montagne, B. Revel, Mater. Chem. Phys. 124 (2010) 732–737.
[21] P. Pascuta, G. Borodi, N. Jumate, I. V-Simiti, D. Viorel, E. Culea, J. Alloys Compd. 504 (2010) 479–483.
[22] N.H. Ray, J. Non-Cryst. Solids 15 (1974) 423–434.
[23] M. Rada, V. Maties, M. Culea, S. Rada, E. Culea, Spectrochim. Acta Part A 75 (2010) 507–510.
[24] K.A. Aly, A. Dahshan, Y.B. Saddeek, J. Therm. Anal. Calorim. 100 (2010) 543–549.
[25] P.S. Prasad, B.V. Raghavaiah, R.B. Rao, C. Laxmikanth, N. Veeraiah, Solid State Commun. 132 (2004) 235–240.
[26] J.-R. Kim, G.-K. Choi, D.K. Yim, J.-S. Park, K.S. Hong, J. Electroceram. 17 (2006) 65–69.
[27] Y.B. Saddeek, Physica B 406 (2011) 562–566.
[28] A. M-Milankovic, A. Santic, A. Gajovic, D.E. Day, J. Non Cryst. Solids 325 (2003) 76–84.
[29] D. Boudlich, M. Haddad, A. Nadiri, R. Berger, J. Kliava, J. Non Cryst. Solids 224 (1998) 135–142.
[30] J. Šubčík, L. Koudelka, P. Mošner, L. Montagn, G. Tricot, L. Delevoye, I. Gregora, J. Non Cryst. Solids 356 (2010) 2509–2516.
[31] J. Šubčík, L. Koudelka, P. Mošner, L. Montagn, B. Revel, I. Gregora, J. Non Cryst. Solids 355 (2009) 970–975.
[32] S.H. Santagneli, C.C. de Araujo, W. Strojek, H. Eckert, J. Phys. Chem. B 111 (2007) 10109–10117.
[33] D. Boudlich, L. Bih, M.E.H. Archidi, M. Haddad, A. Yacoubi, A. Nadiri, B. Elouadi, J. Am. Ceram. Soc. 85 (2002) 623–630.
[34] B.V.R. Chowdari, P.P. Kumari, Solid State Ionics 113–115 (1998) 665–675.
[35] R. Iordanova, L. Aleksandrov, A. Bachvarova-Nedelcheva, M. AtaaLa, Y. Dimitriev, J. Non Cryst. Solids 357 (2011) 2663–2668.
[36] V. Dimitrov, T. Komatsu, J. Solid State Chem. 178 (2005) 831–846.